

Exploring the effect of supramolecular structures of micelles and cyclodextrins on fluorescence emission of local anesthetics†

Emilia Iglesias*

Received 22nd September 2010, Accepted 25th November 2010

DOI: 10.1039/c0pp00286k

Benzocaine (ethyl 4-aminobenzoate, **4**) and its derivatives ethyl 2-aminobenzoate, **2**, and ethyl 3-aminobenzoate, **3**, were found to form association complexes with supramolecular structures of micelles and cyclodextrins (CDs). The fluorescence emission of **2**, **3** or **4** dissolved in the pseudo-micellar phase or included into α -, β -, or γ -CD cavity increases dramatically with respect to that observed in only water. High percentages of organic solvents like dioxane, acetonitrile, DMSO in the aqueous solution lead to a similar effect. The stability constants of the complexes formed between these drugs and cyclodextrins have been determined. In neutral or acid medium, a 1 : 1 stoichiometry for drug : CD complexes have been found, whereas in alkaline medium 1 : 2 stoichiometry was also detected in some cases. Kinetic studies of both the nitrosation of the amine group and the alkaline hydrolysis of the ester function was employed to infer the conformation of the complexes as well as to evaluate their stability constants. Theoretical calculations to optimize the molecular structure of **2**, **3** and **4** allow us to propose possible geometries of the complexes that are in agreement with the experimental data.

Introduction

Benzocaine, ethyl 4-aminobenzoate (**4**), and its derivatives ethyl 2-aminobenzoate (**2**) and ethyl 3-aminobenzoate (**3**) are interesting ester-type local anesthetics (LA) used in pharmaceutical formulations for external and mucous applications, with unique features such as the lack of an amine group ionisable near physiological pH, thus being uncharged substrates. Nevertheless, their parenteral administration is restricted by their limited water solubility.^{1,2} Besides, it is generally believed that interaction of the anesthetic molecules with membrane lipids or membrane proteins leads to the inactivation of neuronal nerve transmission, a key feature on anesthesia mechanism. Therefore, research with anesthetic molecules has two main objectives: first, it is interesting to know their behavior in the presence of membranes and membrane-like environments, and, second, to look for new formulations that control drug delivery in biological systems, prolonging the anesthetic effect and reducing their toxicity or side effects.³

Many biological processes that occur at the surface of biological membranes or within their hydrophobic moiety can be imitated *in vitro* by using simple systems of supramolecular structures (like micelles, cyclodextrins, polymer, DNA, *etc.*). Association of LA to these structures provides a way to increase solubility, stability and bioavailability of drugs.^{4,5} In water above the critical micelle concentration, cmc, self-aggregating surfactants form

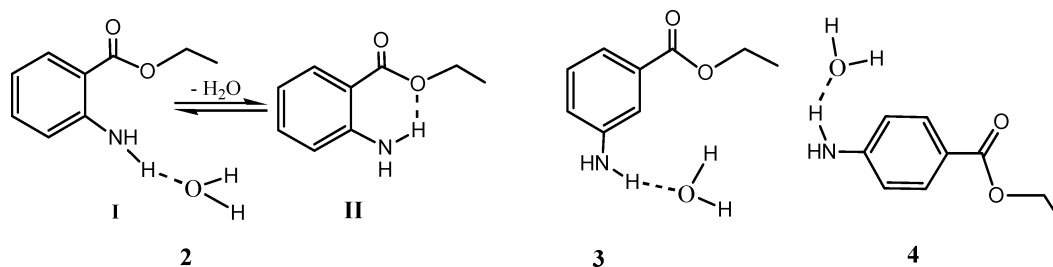
microstructures, such as micelles, that can be used as drug carriers and in the study of the physicochemical properties of membrane-associated drugs.^{6–8} In the same sense, the hydrophobic cavities of cyclodextrins, in combination with their different size, are capable of selectively incorporating organic guest or drug molecules to form inclusion complexes in aqueous solution, which show chemical and spectral properties greatly modified in comparison to that observed in the bulk water phase.^{9–13}

In previous works we have studied the interactions of some local anesthetics, including novocaine, tetracaine and procainamide, with closed environments of micelles and cyclodextrins under different experimental conditions.^{14–16} The common characteristic of these LA is that the amine group is in the *para*-position with respect to the ester (or amide) group. We have found that the most appropriate experimental conditions that yield the highest interaction between the cyclodextrin and the LA correspond to both neutral LA and cyclodextrin, that is, when the van der Waals interactions and the hydrophobic effect that excludes the LA from the bulk water phase reach the maximum level.¹⁴

The aim of this work is the analysis of the effect of both the local anaesthetic geometry and intra- or inter-molecular hydrogen-bonding interactions in the association of drug molecules to closed environments. For that, we have performed a comparative study of the three compounds shown in Scheme 1 in the membrane-mimetic environment existing in micelles or in the cavity of cyclodextrins. The interaction with micellar interfaces of both cationic and anionic micelles has been analysed by fluorescence emission, since it is known that the medium plays an important role in determining the primary photoprocesses of fluorophores in solution. The characterization of the inclusion complexes formed

Departamento de Química Física e E. Q. I. Facultad de Ciencias. Universidad de La Coruña., 15008-La Coruña, Spain. E-mail: qfemilia@udc.es

† Electronic supplementary information (ESI) available: Absorption and emission spectra of compounds **2**, **3**, and **4** dissolved in water, micelles, and CDs; reaction spectra of **2**, **3**, and **4** in water. See DOI: 10.1039/c0pp00286k



Scheme 1 Molecular structures of the local anesthetics.

between **2**, **3**, or **4** and α -, β -, or γ -CD has been performed from either fluorescence or reactivity studies. In acid medium, *i.e.* in conditions of neutral CD host, the nitrosation of the amine group was also investigated; whereas, in alkaline medium, *i.e.* in conditions of anionic CD host, the hydrolysis of the ester group was analysed, too. Different behaviour was observed in acid or in alkaline medium. The results were interpreted on the basis of different guest–host binding modes and supported by theoretical guest-structure optimization

Experimental

Materials

The local anesthetics investigated in this work were of the highest purity available (>99%) and were used without further purification. Solvents of spectrophotometric grade were used as received. Cyclodextrins and surfactants were purchased from Sigma of the maximum purity and used as received. The other reagents, acetic acid, sodium acetate, sodium nitrite, or sodium hydroxide, were commercial products of the maximum purity. The concentration of the aqueous solution of NaOH was determined by titration against standards, whereas the acidity of aqueous buffered solutions was obtained from pH measurements. The reported [buffer] refers to the total buffer concentration.

Methods

The UV-vis spectra and kinetic experiments were recorded with a double beam UV-vis spectrophotometer fitted with thermostatted cell holder at 25 °C. Data acquisition of both UV-vis spectra and kinetics were performed with software supported by the manufacturer and converted to ASCII format for their analysis with common packet programs. Kinetic measurements were performed under pseudo-first order conditions with the local anaesthetic as the limiting reagent; we applied the integration method to record the absorbance–time ($A-t$) data during at least 2.5 half-lives and fit the data to the first-order integrated rate equation, $A_t = A_\infty + (A_0 - A_\infty) \times \exp(-k_0 t)$ by non-linear regression analysis, to obtain the pseudo-first order rate constant, k_0 , and A_∞ (the absorbance at infinite time) and $(A_0 - A_\infty)$ as optimizable parameters. In every experiment perfectly first-order behaviour was observed ($r > 0.9999$).

Steady-state fluorescence measurements were performed with an Aminco-Bowman Series 2 spectrofluorometer at 25 °C. Emission intensity was detected at right angles by exciting optically thin solutions ($A \leq 0.15$ for a 10 mm path length) in the region 270–350 nm. Excitation and emission slits were fixed at 4 and 2 (or 4)

nm, respectively. Data acquisition and analysis of fluorescence spectra were performed with the Fluorescence Data Manager Software supported by Aminco.

Time-resolved fluorescence measurements were performed using the time-correlated single photon counting technique with an Edinburgh Instruments as described in the literature.¹⁷

Results and discussion

1. Studies in homogeneous and microheterogeneous media

Absorption and emission spectra of the three anesthetics have been studied in solvents of various polarities and hydrogen bonding capability. The absorption spectrum of **2**, **3**, or **4** in all solvents, or in water under different acidity conditions, is characterized by two bands; a larger wavelength band (LW) with a maximum around 300 nm and a shorter wavelength band (SW) at 220–240 nm. Both SW and LW bands are ascribed to $\pi \rightarrow \pi^*$ transition of the benzenoid system and suffer small solvent shift. The protonation of H_2N group in, for instance, compound **2** ($pK_a \sim 2.19$)¹⁸ causes a strong decrease in the absorption intensity of the LW, as well as a pronounced blue shift of the SW with respect to the neutral form; Fig. 1a shows representative results. The effect of acids observed with the other two isomers is much smaller; both the absorption and emission wavelength maxima of **2** are largely red shifted in every medium when compared to **3** or **4** because of the intramolecular hydrogen bonding, Fig. 1b. The red shift increases according to the sequence $4 < 3 < 2$, which indicates that the position of the substituent in the phenyl ring is the key factor for the absorption and emission behavior, because of the different electronic densities of the HOMO on each atom. The relevant data are listed in Table 1.

All three compounds give only one broad structureless emission band that shows normal Stokes shift in all solvents. The emitting chromophore is the benzene ring, and emission occurs from the $(\pi, \pi^*)S_1$ state. This fact indicates that the excited and emitting species are the same. Nevertheless, the Stokes shifts observed for **2** are higher than that of **4** (Fig. 1b), due to the intramolecular hydrogen bonding in the former, which stabilizes the excited state.

On the other hand, the larger dipole moment of the excited state than that of the ground state provokes a larger Stokes shift in polar and/or protic solvents, such as water or methanol, than in apolar and/or aprotic solvents such as dioxane. Both excitation and emission spectra of **2** recorded in various solvents are displayed in Fig. 2a. While the fluorescence emission yield in water of both **3** and **4** is practically negligible, the **2** isomer shows a reasonable good fluorescence yield; however, it is strongly

Table 1 Spectroscopic properties of local anesthetics ethyl 2-aminobenzoate, **2**; ethyl 3-aminobenzoate, **3**, and ethyl 4-aminobenzoate or benzocaine, **4**, in different solvents

LA	Absorption spectrum			Emission spectrum				
	Aqueous medium	λ_1/nm ($\log \epsilon$)	λ_2/nm ($\log \epsilon$)	Solvent	ϵ_r^a	$\lambda_{\text{ex}}/\text{nm}$	$\lambda_{\text{em}}/\text{nm}$	Stokes shift/ cm^{-1}
2	neutral ^b	244 (3.89)	326 (3.62)	dioxane	2.21	345	393	3540
	mild acid ^c	243 (3.90)	326 (3.63)	MeCN	35.94	341	395	4010
	strong acid ^d	226 (4.06)	273 (3.07)	DMSO	46.45	349	402	3780
				MeOH	32.66	345	407	4420
				water	78.30	339	422	5800
3	neutral ^b	242	312 (3.36)	dioxane ^e	—	320	406	6620
	mild acid ^c	shoulder	312 (3.33)	MeCN ^e	—	320	409	6800
	strong acid ^d	226 (4.05)	312 (3.01)	DMSO ^e	—	343	418	5230
				water	—	320	460	9510
4	neutral ^b	219 ((4.09)	284 (4.24)	dioxane	2.21	295	328	3410
	mild acid ^c	shoulder	284 (4.24)	MeCN	35.94	295	331	3690
	strong acid ^d	226 (4.18)	275 (3.48)	DMSO	46.45	305	339	3290
				MeOH	32.66	300	346	4430
				water	78.30	305	356	4700

^a Relative dielectric constant. ^b Water. ^c Buffer solution of acetic acid–acetate pH 4.65. ^d HCl 0.04 M. ^e >95% v/v.

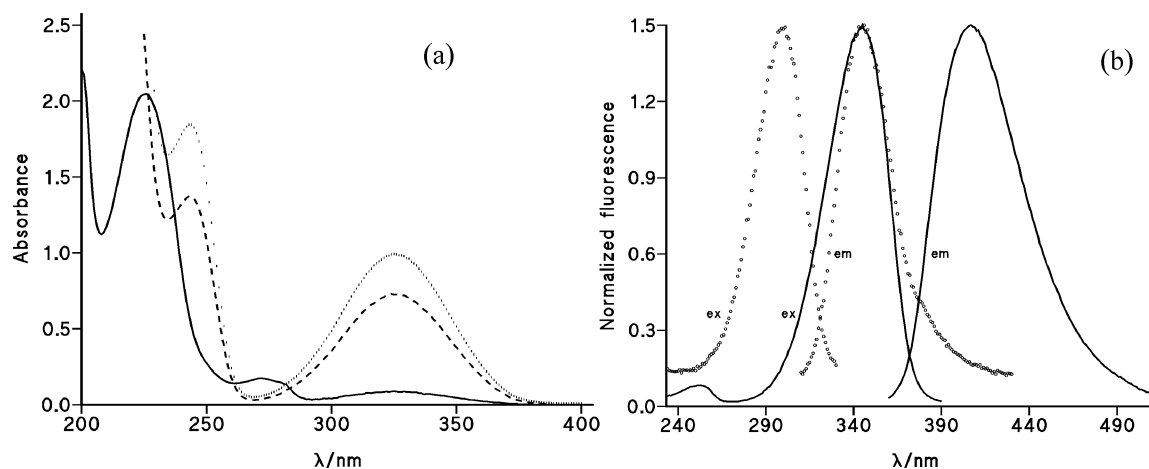


Fig. 1 (a) Absorption spectra of **2** 0.19 mM in (···) neutral medium; (---) mild acid medium of acetic acid–acetate buffer, and in (—) strong acid medium of HCl; (b) normalized fluorescence excitation (ex) and emission (em) spectra of (○) benzocaine and of (—) **2** in methanol. See Table 1 for excitation and emission wavelength values.

enhanced in apolar solvents. Fig. 2b shows comparative results of the fluorescence intensity variation against the solvent percentage for compounds **2**, **3**, and **4** in dioxane, as a representative solvent. These emitting molecules are sensitive to the hydrogen-bonding character of the solvent. The fluorescence intensity of all them increases in going from protic (*e.g.* water) to polar aprotic media (*e.g.* dioxane) as clearly manifest the results of this figure, with drastic effects in benzocaine and in the *meta*-amine isomer. Two different ground-state conformers (I and II of Scheme 1) can be possible for ethyl 2-aminobenzoate, whereas only conformer I is possible in compounds **3** and **4**. However, **2** displays only one emission band and normal Stokes shift, which excluded intramolecular proton transfer in the excited state. The contrary was observed in, for instance, methyl salicylate fluorophore¹⁹ due to the stronger O···H···O intramolecular hydrogen bond. The existence of isomer II in ethyl 2-aminobenzoate contributes to the high fluorescence yield observed in water in comparison to the *meta*- and *para*-amine isomer.

The time-resolved fluorescence of **2** was examined in neutral aqueous medium. Analysis of the fluorescence decay¹⁷ shows good fit to biexponential function affording the lifetimes $\tau_1 = 1.800 \pm 0.004$ ns and $\tau_2 = 6.5 \pm 0.1$ ns with preexponential factors all positive and the relative amplitude as $\alpha_1 = 33 \times 10^{-3}$ (93%) and $\alpha_2 = 1 \times 10^{-3}$ (7%). The two emitting species were attributed to I and II conformers of **2**. The form I predominates, but conformer II is more stable. Attempts to measure the lifetimes of **3** and **4** gave no reliable data due to the low quantum yield observed in water.

The properties of the aqueous medium can also be drastically modified in the presence of micelles that are generated by self-aggregating surfactants to produce microheterogeneous media. For the sake of simplicity, we used both anionic micelles of sodium dodecyl sulfate (SDS) and cationic micelles of tetradecyltrimethylammonium bromide (TTABr) in neutral aqueous medium (no acid or base have been added). Addition of 0.025 M SDS or 0.030 M TTABr very slightly affects the absorption spectrum of

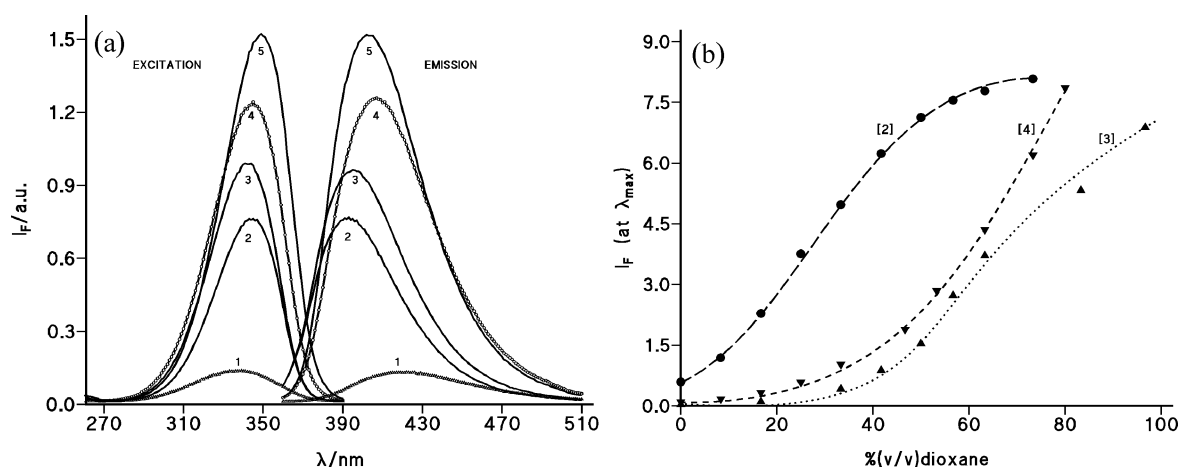


Fig. 2 Excitation and emission spectra of ethyl 2-aminobenzoate 42 μM in different solvents: (a) non-normalized spectra in (1) water, (2) dioxane, (3) acetonitrile, (4) MeOH, (5) DMSO; (b) fluorescence emission intensities as a function of the percentage (v/v) of dioxane in the aqueous solution of compounds 2, ethyl 2-aminobenzoate; 3, ethyl 3-aminobenzoate, and 4, ethyl 4-aminobenzoate.

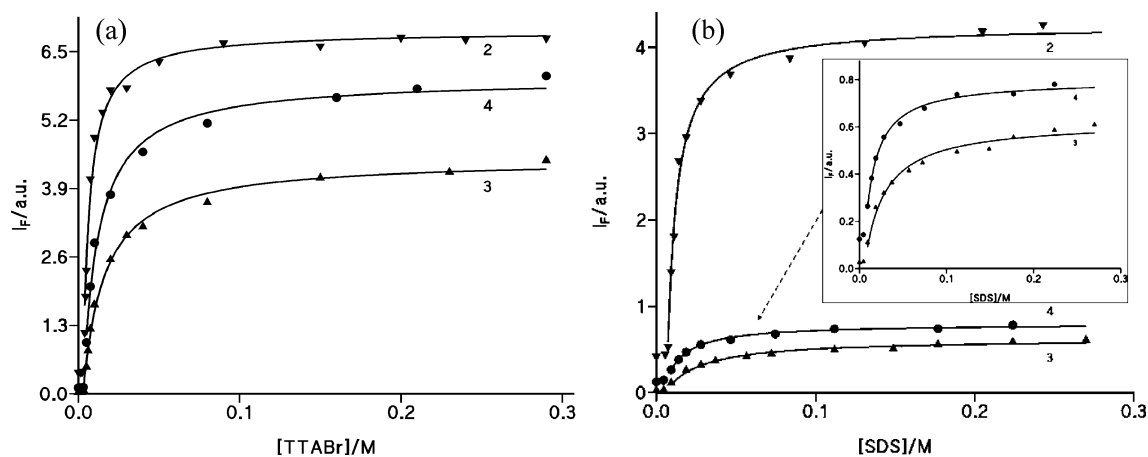


Fig. 3 Plot of fluorescence emission intensities as a function of (a) TTABr concentration and (b) SDS concentration for (∇) ethyl 2-aminobenzoate, 2; (\bullet) benzocaine, 4, and (\blacktriangle) ethyl 3-aminobenzoate, 3. The inset shows the lowest two curves at full y-axis scale.

2, shifting both SW and LW to the red – 4 and 14 nm, respectively, in TTABr, but only 2 and 4 nm, in SDS (Fig. S1 to S3, ESI †); nevertheless, the fluorescence intensity increases strongly and the wavelength emission maxima (λ_{em}) shift to shorter wavelength.

Whatever the surfactant, the emission intensity increases with the surfactant concentration above the cmc (critical micelle concentration). Representative data are displayed in Fig. 3.

The comparison between micellar media and homogeneous media of water-solvent mixtures indicates that, while in micelles the position of the emission maxima (*i.e.*, $\lambda_{\text{em}}^{\text{max}}$) remains invariable as the surfactant concentration increases just above the cmc 20 (e.g. from 5 mM to 0.29 M in TTABr or from 9 mM to 0.27 M in SDS), a gradual blue shift of $\lambda_{\text{em}}^{\text{max}}$ of more than $435 \times 10^3 \text{ cm}^{-1}$ was observed in water-solvent mixtures (Table 2). This fact reflects the drastic difference between homogeneous and microheterogeneous media. Thus, while micellar systems can be considered as composed of particles, usually much smaller than the wavelength of light, that can be seen as hydrophobic pockets with restricted or no access to water molecules, where the fluorophore incorporated and senses a unique microenvironment, in homogeneous media of water-solvent mixtures the nature of

the probe microenvironment is changing parallel to the solvent composition.

Incorporation of LA into micelles can be treated as the partitioning between two phases: the micelles, being visualized as the micellar pseudo-phase, and the bulk water phase, according to the equilibrium process $\text{LA}_w + \text{Dn} \rightleftharpoons \text{LA}_m$ with K_m representing the binding constant of LA to micelles (Dn refers to the micellized surfactant). The LA dissolved in the aqueous micellar pseudo-phase displays similar absorption spectrum as that observed in water; hence, the excitation wavelength neither changes significantly; however, both excitation and emission spectra were recorded in every case to find the optimal conditions. By contrast, the fluorescence emission intensities in both water and micellar phases, that is I_w and I_m respectively, would differ significantly because, on fluorescence time scales, micelles can be considered as rigid host systems carrying the solubilized fluorophore molecules, where the lifetimes (τ) and/or fluorescence yields (ϕ) are different, mainly due to the strong reduction of solvent quenching. As benzocaine and its 2 and 3 isomers are freely moving non-covalently-bound fluorophores, it is envisaged that both parameters increase in the micellar pseudo-phase. Therefore,

Table 2 Maximum wavelength of fluorescence emission and the corresponding intensities measured as a function of the dioxane percentage in the binary aqueous mixtures and as a function of the surfactant concentration in the aqueous micellar medium, showing the progressive blue shift in homogeneous media, but the sharp shift in micelles

Homogeneous solvent of dioxane/water mixtures (ethyl 3-aminobenzoate, 3)			Microheterogeneous solvent: aqueous micellar medium (ethyl 2-aminobenzoate, 2)		
% Dioxane (v/v)	$\lambda_{\text{em}}^{\text{max}}/\text{nm}$	$I_{\text{F}}/\text{a.u.}$	[SDS]/M	$\lambda_{\text{em}}^{\text{max}}/\text{nm}$	$I_{\text{F}}/\text{a.u.}$
0	457	0.038	0	421	0.446
16.7	453	0.142	7.47×10^{-3}	421	0.541
33.3	445	0.530	9.33×10^{-3}	414	1.416
42.0	441	1.059	0.014	414	2.692
50.0	437	1.758	0.028	414	3.378
63.0	431	3.933	0.240	414	4.187
83.3	421	6.877			
96.7	406	8.527	[TTABr]/M	$\lambda_{\text{em}}^{\text{max}}/\text{nm}$	$I_{\text{F}}/\text{a.u.}$
			0.240	409	6.728

Table 3 Experimental conditions and fluorescence intensities measured in water, I_{w} , and optimized values in cationic micelles of TTABr and anionic micelles of SDS, I_{m} , along with the association constant of the local anesthetic (LA) to micelles, K_{m} , eqn (1)

LA (c/μM)	$\lambda_{\text{ex}}/\lambda_{\text{em}}$ (nm)	$I_{\text{w}}/\text{a.u.}$	$I_{\text{m}}/\text{a.u.}$	$K_{\text{m}}/\text{dm}^3 \text{ mol}^{-1}$	$\phi_{\text{m}}/\phi_{\text{w}}$
TTABr (tetradecyltrimethylammonium bromide, cmc 3.5 mM) ²⁰					
2 (13.5)	350/409	0.406	6.85 ± 0.10	250 ± 19	17
3 (13.6)	340/434	0.0195	4.41 ± 0.07	79 ± 6	23
4 (15.7)	300/343	0.1124	6.00 ± 0.10	103 ± 9	53
SDS (sodium dodecylsulfate, cmc 7.5 mM) ²⁰					
2 (13.5)	350/413	0.420	4.31 ± 0.07	140 ± 10	10
2 (13.5) buffer ^a	350/413	0.470	3.73 ± 0.07	145 ± 14	8
3 (13.6)	326/443	0.028	0.622 ± 0.017	43 ± 5	22
4 (15.7)	300/347	0.143	0.797 ± 0.010	75 ± 5	6

^a Aqueous solution of acetic acid acetate 0.033 M pH 4.55

the enhancement of emission intensity as a function of [surfactant] is due to different lifetimes of the fluorophore in water ($I_{\text{w}} \propto \phi_{\text{w}}[\text{LA}]_{\text{w}}$), at 100% incorporation in micelles ($I_{\text{m}} \propto \phi_{\text{m}}[\text{LA}]_{\text{m}}$), and at intermediate micelle concentration, ($I_{\text{F}} \propto \phi_{\text{w}}[\text{LA}]_{\text{w}} + \phi_{\text{m}}[\text{LA}]_{\text{m}}$).

The experimental values of I_{F} measured at each [surfactant] and depicted in Fig. 3, show a sharp increase at low surfactant concentration just above the cmc and levels off at high surfactant concentration. Solid lines were drawn by applying eqn (1), where $[\text{Dn}] = [\text{surfactant}] - \text{cmc}$ represents the micellized surfactant concentration. Using non-linear regression analysis, the best fitting values of I_{m} and K_{m} were determined and are listed in Table 3, along with the experimental conditions. The ratio $I_{\text{m}}/I_{\text{w}}$ equals the ratio of the fluorescence quantum yield of the bound (ϕ_{m}) and free molecule (ϕ_{w}); the corresponding enhancement ratio is listed also in Table 3.

$$I_{\text{F}} = \frac{I_{\text{w}} + I_{\text{m}}K_{\text{m}}[\text{Dn}]}{1 + K_{\text{m}}[\text{Dn}]} \quad (1)$$

Even though the fluorescence emission measured in water, I_{w} , is quite different for **2**, **3**, and **4** compound (being $I_{\text{w}(\text{3})} \ll I_{\text{w}(\text{4})} \ll I_{\text{w}(\text{2})}$ following the ratio of 1 : 6 : 21 approximately), the values measured in the micellar pseudophase, I_{m} , follows the same trend but, by contrast, reach quite close levels (the ratio is 1 : 1.4 : 1.6); in other words, micelles enhance the fluorescence quantum yield and the enhancement is higher in TTABr than in SDS micelles.

As neither compound can specifically interact with TTABr micelles (for instance, by electrostatic or H-bonding forces), the

different I_{m} values obtained at 100% incorporation of the drug should reflect different locations inside the micelle, *i.e.* for the same micelle hydrophobicity, the experimental differences must be attributed to the fluorescence probe. In this respect, the **2** isomer is more hydrophobic than the others two due to intramolecular H-bonding. Therefore, this compound resides deeper inside the micellar interface where it senses a less polar environment. The higher value of K_{m} measured for isomer **2** corroborates this statement and is also supported by larger wavelength shift of the LW absorption than that observed with **3** or **4** (Fig. S4, ESI[†]). The peculiar geometry of **4** allows it to enter lengthwise among the surfactant monomers in the micelle with a significant degree of protrusion; which makes the aromatic ring sense an apolar microenvironment. However, the isomer **3** must reside outside in the micellar interface in order to avoid strong disruption of the micelles due to the bulky geometry of this molecule; in fact, the corresponding association constant takes the smallest value of the three LA. Even though, in the case of **4** its molecular geometry facilitates good association to micelles, the interactions (H-bonding) with water molecules reduce incorporation to micelles; the observed results are the balance of all these driving forces.

The situation observed with anionic micelles of SDS is quite different for compound **2** in comparison to **3** and **4**. The possibility of H-bonding formation between the sulfate head groups ($-\text{O}-\text{SO}_3^-$) of the surfactant monomers and the amino group of the fluorophore, forces compounds **3** and **4** to reside probably in the micellar interface, outside the Stern-layer; on the contrary,

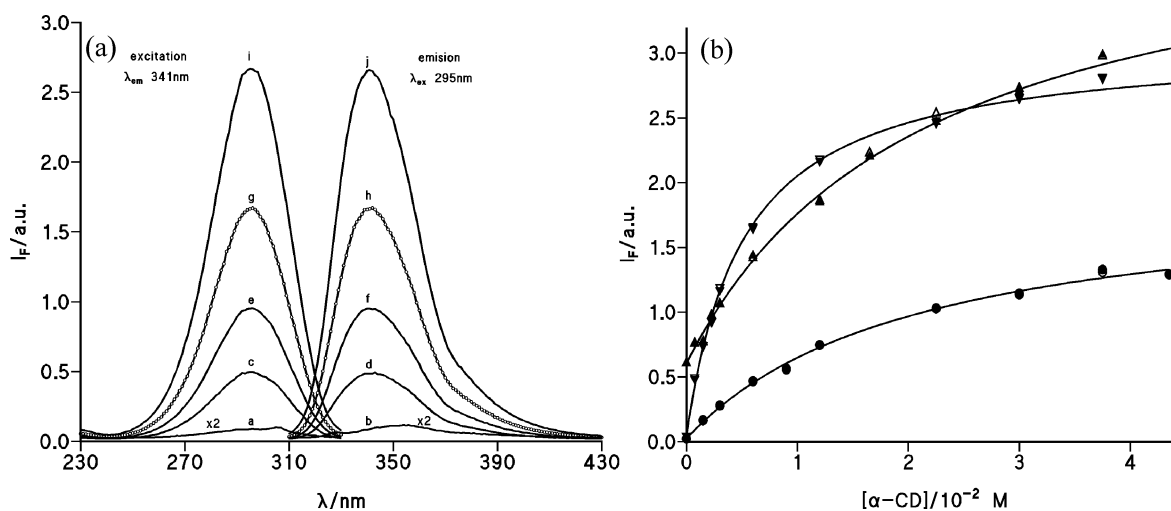


Fig. 4 (a) Excitation and emission spectra of **4** as a function of α -CD concentration. Scans *a* and *b* were recorded in the absence of CD and the intensity was amplified by a factor of 2; the next scans were recorded at [CD] equal to: (*c,d*)0.75; (*e,f*)2.25; (*g,h*)6.0, and (*i,j*)30 mM. (b) Variation of the emission intensity as a function of α -CD for (\blacktriangle) **2**, 10.6 μ M; (\bullet) **3**, 46.7 μ M; and (\blacktriangledown) **4**, 9.2 μ M. Conditions in Table 4.

the intramolecular H-bonding that is possible in compound **2**, allows this compound to incorporate more inside the micelle. Nevertheless, if one observes the data in Table 2, the comparison of the results measured in 0.24 M or either [SDS] or [TTABr], indicates that, firstly, the emission intensity in SDS ($I_m = 4.2$) is quite lower than that measured at the same [TTABr] ($I_m = 6.7$), and secondly, the emission maxima in SDS ($\lambda_{em} = 414$ nm) is red shifted with respect to TTABr ($\lambda_{em} = 409$ nm). Both observations reflect the more hydrophobic microenvironment sensed by **2** in TTABr micelles than in SDS micelles. These results evidence the drastic differences in homogeneous and microheterogeneous media, as well as the importance of the molecular structure of the LA and the nature of the interface in the magnitude of mutual interaction.

The time-resolved fluorescence of **2** was examined in aqueous micellar medium of 0.025 M SDS and 0.030 M TTABr, that is, according to Fig. 3, in a region where the I_F reaches almost the maximum value. Global deconvolution analysis of the two time profiles afforded a good fit ($\chi^2 < 1.1$) on the basis of a biexponential function with lifetimes $\tau_1 = 2.28 \pm 0.08$ ns (5.7%) and $\tau_2 = 9.01 \pm 0.015$ ns (94.3%) in SDS micelles and $\tau_1 = 1.4 \pm 0.1$ ns (1.3%) and $\tau_2 = 10.20 \pm 0.01$ ns (98.7%) in TTABr micelles. The comparison with the results obtained in water indicates that the longer-lived component in the emission, which is the most affected by the presence of micelles and attributed to the II-form of **2**, is the main species in micellar media.

2. Studies in aqueous cyclodextrin solutions

A third common way to alter the structure of water solvent is the addition of cyclodextrins. In aqueous solutions, the non-polar cyclodextrin cavity is occupied by water molecules, which can be readily replaced by appropriate guest molecules of lower polarity than water. The driving forces leading to the inclusion complexation of cyclodextrins were thought to include electrostatic, van der Waals, hydrophobic effect and hydrogen-bonding interactions.²¹ Upon inclusion into the CD cavity, the chemical and spectral properties of the guest can be affected. The hydrophobic

microenvironment of the CD cavity enhances the fluorescence²²⁻²⁴ and decreases the reactivity of the included guest,²⁵ except when the reaction was CD mediated.²⁶

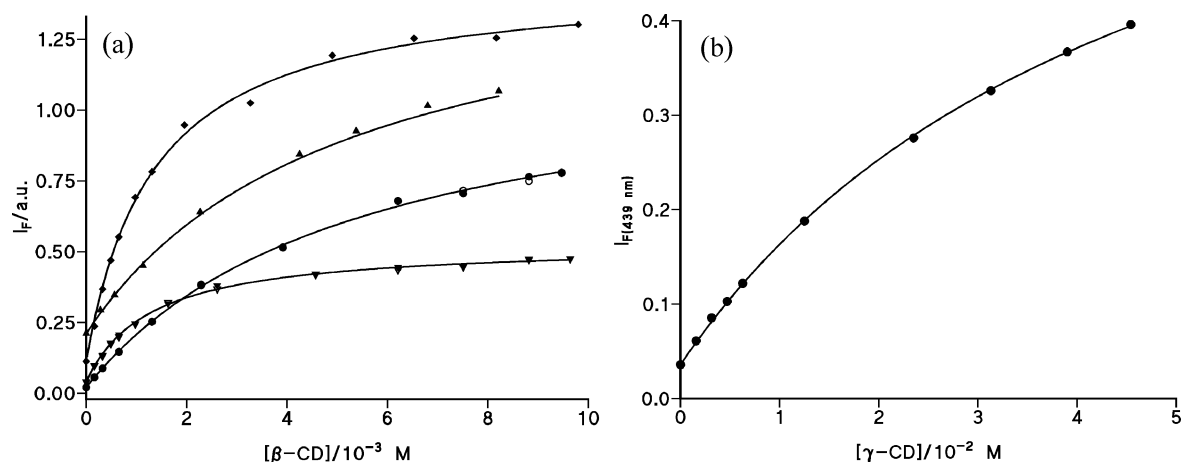
The absorption spectrum of **2**, **3** or **4**, recorded in the presence of cyclodextrins (Fig. S1 to S3, ESI[†]), shows small red shift in λ_{max} (<4 nm) and no significant absorbance changes for a reliable evaluation of their interaction with the CD cavity. By contrast, the emission spectra show strong variation in the presence of cyclodextrins; in the same manner, the reactivity of the amine group towards nitrosation or the hydrolysis of the ester function is notably affected in aqueous cyclodextrin solutions.

2.1 Fluorescence measurements. The fluorescence intensity in water of the local anesthetics of Scheme 1 increases gradually upon addition of either α -, β -, or γ -CD, due to the enhanced dissolution of the guest into the hydrophobic CD cavity, which indicates the formation of inclusion complexes. The excitation and emission spectra of **4** recorded as a function of α -CD concentration are shown in Fig. 4a. Similar spectra were obtained in any other possible combination of **2**, **3**, and **4** and α -, β -, or γ -CD. Fig. 4b and 5 display representative plots (of nine possible combinations) of emission intensity, I_F , against [CD].

Under experimental conditions of neutral CD, these plots describe saturation curves at high CD concentration. This fact suggests the formation of 1 : 1 inclusion complexes. In this sense, the stoichiometry of the benzocaine, **4**, and β -CD complex was determined by Job-plot analysis²⁷ as being 1 : 1.²⁸ However, the most general means for assessing stoichiometry is the constancy of stability constants as the host concentration is varied, that is, the success of an assumed stoichiometry model in accounting for the data. This procedure is followed in the quantitative treatment of the following experimental data. Then, assuming the formation of 1 : 1 inclusion complex between the LA and CD according to eqn (2), and taking into account that $[CD]_0 \gg [LA]_0$ (*i.e.* the total CD concentration is much higher than that of the LA), along with the mass balance on host $[CD]_0 \approx [CD]_{free}$ and guest $[LA]_0 = [LA_w] + [LA-CD]$, and the stability constant K_{11} , it can be easy to arrive

Table 4 Experimental conditions and fluorescence intensities measured in water, I_w , and optimized values in cyclodextrins, I_c , along with the stability constant of the 1 : 1 inclusion complex formed between local anesthetic (LA) and cyclodextrins, K_{11} (eqn (2) and (3))

LA ([LA])	Cyclodextrin	$\lambda_{ex}/\lambda_{em}$ (nm)	$I_w/a.u.$	$I_c/a.u.$	$K_{11}/dm^3 mol^{-1}$	ϕ_c/ϕ_w
2 (10.6 μ M)	α -CD	342/410	0.604 ± 0.030	4.2 ± 0.1	50 ± 3	7
	β -CD	343/410	0.723 ± 0.050	6.6 ± 0.1	184 ± 7	9
	γ -CD	343/417	0.580 ± 0.035	5.3 ± 0.5	73 ± 15	9
3 (46 μ M)	α -CD	322/418	0.024	1.96 ± 0.08	48 ± 5	82
	β -CD	325/427	0.021	1.22 ± 0.03	185 ± 9	58
	γ -CD	326/439	0.036	0.770 ± 0.015	21.0 ± 0.07	21
4 (9.2 μ M)	α -CD	295/341	0.043	3.09 ± 0.04	194 ± 9	72
	β -CD	300/345	0.048	0.529 ± 0.005	780 ± 30	11
	γ -CD	300/345	0.048	0.257 ± 0.004	60.0 ± 1	5.3
4 (27 μ M)	β -CD	302/346	0.113	1.46 ± 0.02	740 ± 30	13
4 (5 to 14 mM)	β -CD	Phase solubility measurements ²⁸			549 ± 42	

**Fig. 5** (a) Variation of emission of fluorescence intensity as a function of β -CD concentration for **4** (∇) 9.2 μ M and (\blacklozenge) 27 μ M; (\bullet) **3**, 46.7 μ M and (\blacktriangle) **2**, 10.6 μ M. The excitation and emission wavelength are reported in Table 4; (b) Increase of the emission of fluorescence at 439 nm (λ_{ex} , 326 nm) of **3**, 46 μ M, as a function of γ -CD concentration.

at eqn (3) to express the fluorescence intensity of the guest as a function of cyclodextrin concentration. In this equation, I_w and I_c refer to the emission intensity in water and at 100% complexed with CD, respectively.



Fluorescence measurements applied to the determination of stability constants are based on the proportionality of fluorescence intensity to fluorophore concentration, where the proportionality constant includes the quantum yield and the molar absorptivity, ϵ_{ab} . Both parameters, but mainly the quantum yield, take different values for the free (ϕ_w) and included (ϕ_c) guest, *i.e.*, $I_w = \delta_w[LA]_0$ and $I_c = \delta_c[LA \cdot CD]_t$, with $\delta_i = \epsilon_{ab}\phi_i$.

$$I_F = \frac{I_w + I_c K_{11}[CD]}{1 + K_{11}[CD]} \quad (3)$$

The non-linear regression analysis of the experimental data by means of eqn (3), affords the optimized values of the unknown parameters I_c and K_{11} that are collected in Table 4, along with the ratio ϕ_c/ϕ_w that shows the effect of CD on the emission quantum yield.

The guest **2** complexed with whatever CD is very protected from water molecules; in fact, I_c values are comparable to those obtained in solvents or in cationic micelles of TTABr. On the other hand, the complexes formed with β -CD are more stable than that formed with α -, or γ -CD, probably due to both the tight fitting of **2** to the CD cavity and to the gain in energy when high energetic water molecules inside the β -CD are replaced by the hydrophobic guest.

Benzocaine and the guest **3** hardly show fluorescence in water as a consequence of the very fast radiationless decay, thus no intramolecular hydrogen-bonding is possible; but, the presence of CDs enhances strongly the fluorescence emission. The highest effect was observed in α -CD solutions and following the trend: $I_c(\alpha\text{-CD}) > I_c(\beta\text{-CD}) > I_c(\gamma\text{-CD})$ with increasing factors of 80 : 50 : 18 for the case of **3** and of 70 : 13 : 5 for the case of **4**. These results reflect that the fluorophore moiety of **3** and **4** remains very exposed to water molecules; the effect is very marked in benzocaine, which, in spite of forming the most stable complexes with whatever CD, the I_c values are very low in comparison to that obtained in solvents or, for instance, in cationic micelles.

For the sake of comparison, Table 4 also includes the stability constant of the inclusion complex formed between **4** and β -CD determined from solubility measurements.²⁸ The datum

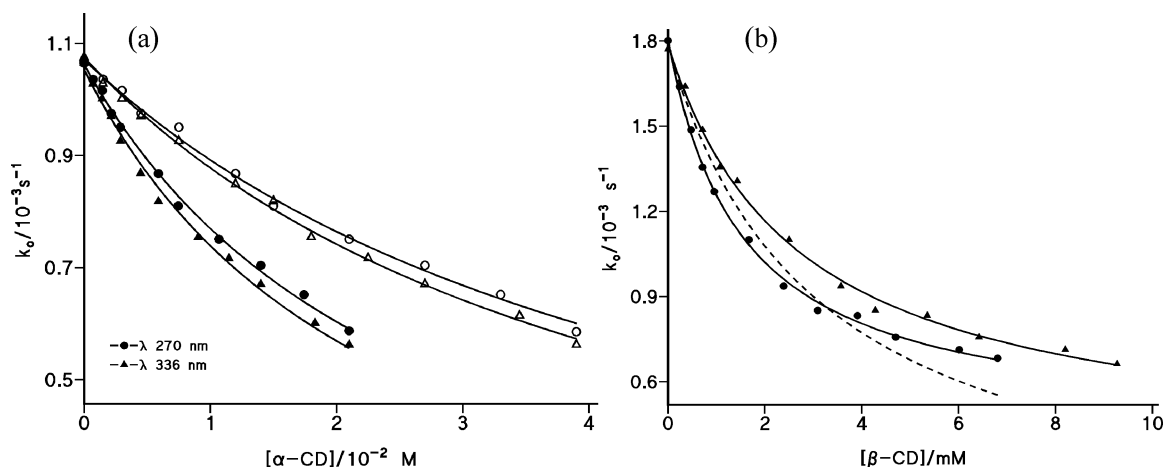


Fig. 6 Plot of k_o against cyclodextrin concentration obtained in the nitrosation of (a) ethyl 2-aminobenzoate, **2**, in the presence of α -CD followed the increase in absorbance at (\circ , \bullet) 270 nm or the decrease in absorbance at (Δ , \blacktriangle) 336 nm; open points represent total cyclodextrin concentration; solid points represent free cyclodextrin concentration; (b) benzocaine in the presence of β -CD at [nitrite] = 2.9 mM, [buffer] = 0.078 M, pH 4.50, (\blacktriangle) k_o against total [β -CD]; (\bullet) k_o against free [β -CD]; dashed line, fitting to eqn (4) with the assumption $k_c = 0$.

($K_c = 549 \text{ M}^{-1}$) is significantly lower than that obtained in this work. The sensibility of fluorescence determinations is notably higher and the required amount of guest is considerably lower, which leads to more accurate results.

The time-resolved fluorescence of **2** was measured in 30 mM α -CD and 7.0 mM β -CD. In both cases, a bi-exponential decay with lifetimes $\tau_1 = 2.29 \pm 0.03 \text{ ns}$ (18.6%) and $\tau_2 = 8.43 \pm 0.02 \text{ ns}$ (81.4%) in α -CD and $\tau_1 = 2.02 \pm 0.04 \text{ ns}$ (8.9%) and $\tau_2 = 9.26 \pm 0.01 \text{ ns}$ (90.1%) in β -CD were observed. Against, the longer lifetime, which corresponds to the emitting conformer II, is the main species in the presence of cyclodextrins and that which is included into the CD cavity.

2.2 Reactivity measurements. In order to postulate a more exact picture of the conformation of inclusion complexes, we studied the effect of cyclodextrins on the reactivity of the guest towards the nitrosation of the amine group in mild acid medium and the alkaline hydrolysis of the ester group. The results could inform us of the position of these reactive groups in the CD complexes.

Nitrosation in acid medium. The influence of CDs on the nitrosation of the primary amine group of benzocaine, **4**, and of ethyl 2-aminobenzoate, **2**, has been analyzed in aqueous buffered medium of acetic acid–acetate ([buffer] = 0.075 M) at pH \sim 4.50. The nitrosation of ethyl 3-aminobenzoate, **3**, resulted complicated by products phase separation (strong turbidity).

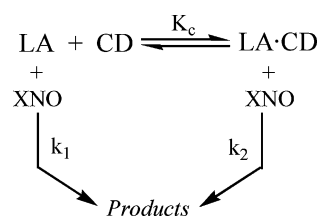
The reaction spectra of **2**, recorded from 240 to 400 nm at [2] = $1.5 \times 10^{-4} \text{ M}$ and [nitrite] = $2.9 \times 10^{-3} \text{ M}$, shows two broad bands centered at 327 and 270 nm. The former decreases with time meanwhile the absorption maximum shifts to 311 nm, whereas the later increases with time; the spectral changes describe two well-defined isosbestic points at 311 and 251 nm (Fig. S5, ESI†). The reaction was followed at both 336 (decrease in absorbance, $\Delta\epsilon \sim 3300 \text{ mol}^{-1} \text{ dm}^3 \text{ cm}^{-1}$) and 270 nm (increase in absorbance, $\Delta\epsilon \sim 7300 \text{ mol}^{-1} \text{ dm}^3 \text{ cm}^{-1}$). Under the same experimental conditions, the observed rate constant takes the same value independent of the wavelength used to follow the reaction, which indicates both changes correspond to the same reaction process.

The reaction spectra of **4**, recorded also between 240 and 400 nm at [4] = $9 \times 10^{-5} \text{ M}$ and [nitrite] = $2.9 \times 10^{-3} \text{ M}$, show a broad band centered at 283 nm that decreases with time and shifts the absorption maximum to 263 nm, by drawing also two well-defined isosbestic points at 318 and 271 nm (Fig. S5, ESI†). We have chose $\lambda = 290 \text{ nm}$ ($\Delta\epsilon \sim 14000 \text{ mol}^{-1} \text{ dm}^3 \text{ cm}^{-1}$) to follow the reaction.

The observed rate constant, k_o , obtained for either **2** or **4** decreases as the cyclodextrin concentration increases. Representative plots of k_o versus [CD] are given in Fig. 6. Taking into account that the nitrosating agents XNO (formed from the HNO_2 according to the equilibrium reactions $\text{HNO}_2 + \text{X}^- + \text{H}^+ \rightleftharpoons \text{X-NO}$, K_1 , or $2\text{HNO}_2 \rightleftharpoons \text{N}_2\text{O}_3$, $K_2 = 3 \times 10^{-3} \text{ M}^{-1}$ at 25°C ²⁹) are highly hydrophilic species, the complexation process leads to the reactant separation; in other words, the LA included into the CD cavity is protected from the attack of XNO in water, with XNO being H_2NO^+ , AcNO or N_2O_3 . The degree of encapsulation of H_2N group will determine the possible attack of the nitrosating agent.

The overall reaction mechanism is that of Scheme 2, in which we consider different reactivities for free (k_w) and complexed (k_c) guest, the concentration of both are related by the equilibrium constant, K_c , with LA representing to either **2** or **4**. The mass balance of $[\text{LA}]_i = [\text{LA}] + [\text{LA}\cdot\text{CD}]$ ($[\text{LA}] \ll [\text{CD}]$) leads to eqn (4), where $k_w = k_1[\text{XNO}]$ and $k_c = k_2[\text{XNO}]$.

$$k_o = \frac{k_w + k_c K_c [\text{CD}]}{1 + K_c [\text{CD}]} \quad (4)$$



Scheme 2 Equilibrium and reaction steps in nitrosation.

The k_o vs. [CD] profiles obtained in the nitrosation of **2** fit perfectly to eqn (4) if $k_c = 0$, i.e. the complex formed between **2**

Table 5 Experimental conditions and results obtained in the nitrosation of **2** and **4** in aqueous buffered solutions of acetic acid–acetate, [buffer] = 0.075 M of pH 4.50, in the presence of cyclodextrins. See Scheme 2 and eqn (4) for the interpretation of rate constants

LA (c/M)	Cyclodextrin	[nitrite]/M	λ/nm ($\Delta\epsilon/\text{M}^{-1}\text{cm}^{-1}$)	$k_w/10^{-3}\text{ s}^{-1}$	$k_c/10^{-3}\text{ s}^{-1}$	K_c/M^{-1}	$K_c^{\text{ap}}/\text{M}^{-1}$
2 (1.5×10^{-4})	α -CD	2.9×10^{-3}	270 (7300)	1.06	~ 0	40.80 ± 0.95^a	21.0 ± 0.5
	α -CD	2.9×10^{-3}	336 (3200)	1.05	~ 0	42.5 ± 1.0^a	22.9 ± 0.7
	β -CD	3.5×10^{-3}	270 (7300)	1.57	~ 0	182 ± 2^b	131 ± 2
4 (0.9×10^{-4})	α -CD	2.9×10^{-3}	290 (14000)	1.42	(0.35 ± 0.03)	160 ± 10^a	61 ± 3
	β -CD	3.5×10^{-3}	290 (14000)	1.78	(0.41 ± 0.02)	684 ± 20^b	370 ± 20
	γ -CD	3.5×10^{-3}	290 (14000)	1.85	(0.34 ± 0.05)	65 ± 6^c	45.5 ± 3.0

^a The value of K_1 used to calculate the free cyclodextrin concentration was 15 M^{-1} . ^b $K_1 = 5\text{ M}^{-1}$. ^c $K_1 = 4\text{ M}^{-1}$.

and α - or β -CD is unreactive. The amine group must be completely protected from the attack of the nitrosating agent. By contrast, the k_o vs. [CD] profiles obtained in the nitrosation of **4** fit to eqn (4) with significant values of k_c , the rate constant for the nitrosation of the complex. The dashed line in Fig. 6 was drawn by assuming $k_c = 0$. The determined values of both k_c and K_c , along with the experimental conditions, are collected in Table 5.

The optimized values of K_c are significantly lower than that obtained from fluorescence measurements in pure water (compare data in Tables 4 and column 8 of Table 5). Obviously, K_c values must be independent of the method used to evaluate them. Nevertheless, there is an important difference in the experimental conditions of nitrosation experiments that refer to the presence of acetic acid and acetate ions ([buffer] = 0.075 M). Both components of the buffer form inclusion complexes with CDs;^{21,30} then, the K_c values obtained in the fitting of k_o against total CD concentration are, in fact, K_c^{ap} (apparent values modified by the competition of the buffer for the CD cavity). By representing HAc or Ac⁻ by I, then $\text{I} + \text{CD} \rightleftharpoons \text{I-CD}$, K_1 , the mass balance on $[\text{I}]_0 = [\text{I}] + [\text{I-CD}]$ and on $[\text{CD}]_0 = [\text{CD}] + [\text{I-CD}]$ leads to eqn (5) to determine the free cyclodextrin concentration, [CD].

$$[\text{CD}]^2 + [\text{CD}] \left([\text{I}]_0 + \frac{1}{K_1} - [\text{CD}]_0 \right) - \frac{[\text{CD}]_0}{K_1} = 0 \quad (5)$$

Solving this quadratic equation for each initial $[\text{CD}]_0$, one determines the corresponding free cyclodextrin concentration. For that, we assumed the K_1 reported in Table 5.³⁰ The plot of k_o vs. free [CD] is also shown in Fig. 6. The corresponding fit to eqn (4) yields the values of K_c reported in Table 5. As can be seen, the comparison with those obtained from fluorescence (Table 4) is now in very good agreement.

However, the most important observation of nitrosation results is that the inclusion complex of **4** reacts with the nitrosating agent at reaction rates 4-fold lower than that of uncomplexed compound, whereas those of **2** do not. This fact indicates that in the inclusion complexes of benzocaine, the amine group remains exposed to water, a result that confirms the fluorescence I_c values, which are much lower than those read in solvents or in cationic micelles. By contrast, in the inclusion compounds of **2** the amine group is not exposed to water molecules.

Hydrolysis in alkaline medium. The alkaline hydrolysis of the ester function of **2**, **3**, or **4** compound was studied in aqueous solutions of cyclodextrins at high and fixed $[\text{OH}^-]$, to ensure the ionization of secondary OH-group of cyclodextrins ($\text{p}K_a =$

12.33; 12.20, and 12.08 respectively to α -, β -, and γ -cyclodextrin at $25\text{ }^\circ\text{C}$)³¹ and also to obtain adequate reaction rates. Therefore, under these experimental conditions, the cyclodextrins are negatively charged.

The LW absorption band displayed in the spectra of **2**, **3**, or **4** (with maxima at 327, 311, and 285 nm, respectively; Table 1) decreases with time in alkaline medium meanwhile shifts to shorter wavelength and fixed, at the end of the reaction, at 309, 302 and 265 nm, respectively, by describing, in each case, two isosbestic points centered, for instance, at 270 and 232 nm in the benzocaine hydrolysis (Fig. S6 and S7, ESI[†]). Therefore, a clean reaction occurs to give, as the reaction products, 2-, 3-, or 4-aminobenzoate and ethanol, respectively to the hydrolysis of **2**, **3**, or **4**.

The reaction kinetic was studied by recording the decrease in absorbance as a function of time at 350 ($\log \epsilon = 3.30$), 330 ($\log \epsilon = 3.0$), and 300 nm ($\log \epsilon = 4.0$), respectively to **2**, **3**, or **4**. The compound **3** hydrolyses nearly 10-fold faster than the other two, due to the inductive effect of the amine group in either *ortho* or *para* positions of the benzoic moiety reduces the electrophilic character of the carbonyl group by resonance effects.

Addition of cyclodextrins to the reaction medium results in a progressive reduction of pseudo-first order rate constant. The k_o vs. [CD] profiles describe saturation curves. Fig. 7 shows representative results. Considering the same CD, the inhibition effect is stronger for benzocaine than for the other two LA, which show similar reduction effect; considering the same LA and different molecular receptor, a concentration of β -CD near 4-fold lower than that of α - or γ -CD yields similar inhibition effect.

The k_o vs. [CD] profiles can be fitted to the overall eqn (6), derived from Scheme 3, with some modifications depending on the LA being considered. In this equation, k_w and k_c represent the pseudo-first order rate constants for the hydrolysis of free and complexed LA; K'_{11} and K'_{12} are the stability constants of the inclusion complexes for 1 : 1 and 1 : 2 stoichiometries, formed between the LA and ionized cyclodextrin, and $[\text{CD}^-]$ represent the stoichiometric ionized CD. The non-linear regression analysis of the experimental data by means of eqn (6) leads to the results of Table 6.

$$k_o = \frac{k_w + k_c K'_{11} [\text{CD}^-]}{1 + K'_{11} [\text{CD}^-] + K'_{11} K'_{12} [\text{CD}^-]^2} \quad (6)$$

Inclusion complexes of **2** appear unproductive, irrespective of the cyclodextrin being considered, *i.e.* $k_c \sim 0$ in every case, and with α - and γ -CD the best fit was obtained if both 1 : 1 and 1 : 2

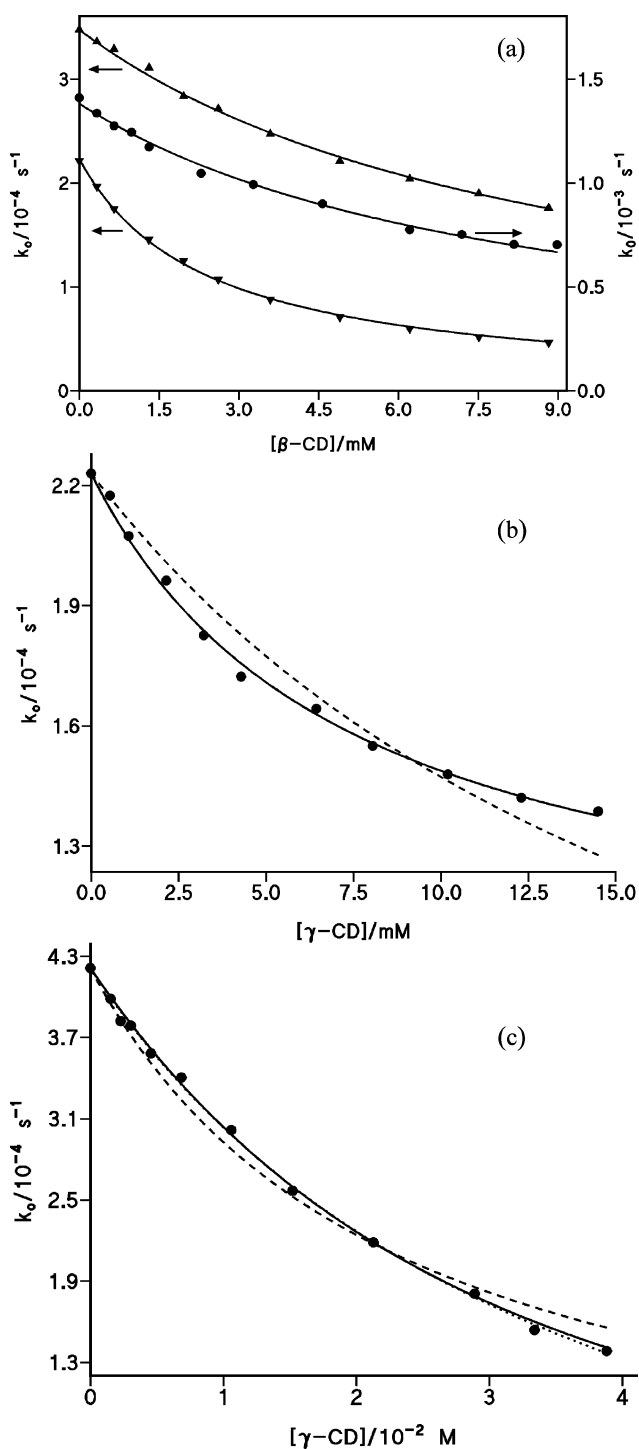
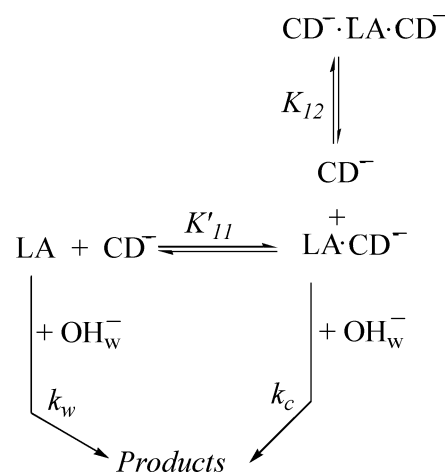


Fig. 7 (a) Influence of β -CD on the basic hydrolysis of (\blacktriangle) **2**, $[\text{OH}^-] = 0.078 \text{ M}$, (\bullet) **3** $[\text{OH}^-] = 0.048 \text{ M}$, right y-axis, and (\blacktriangledown) **4**, $[\text{OH}^-] = 0.083 \text{ M}$, and variation of k_o against $[\gamma\text{-CD}]$ obtained in the alkaline hydrolysis of (b) **4** at $[\text{OH}^-] = 0.075 \text{ M}$; the dashed line shows the calculated points if $k_c = 0$ (unproductive complex), and (c) **2** at $[\text{OH}^-] = 0.095 \text{ M}$; lines show the fits to eqn (6) when $k_c = 0$ (—); when $K_{12} = 0$ but k_c is negative, $k_c = (-1.4 \pm 0.2) \times 10^{-4} \text{ s}^{-1}$, which has no sense (\cdots); and when k_c and K_{12} are zero (---). The results reported in Table 6 correspond to the solid lines.

complexes are considered, in other words both K'_{11} and K_{12} are significant. However, different models have been essayed for this particular case, including the formation of only 1 : 1 unproductive



Scheme 3 Equilibrium and reaction steps in alkaline hydrolysis.

($k_c = 0$) or productive ($k_c \neq 0$) complexes; as $[\mathbf{2}] = 0.5 \text{ mM}$ is much lower than that of α - and γ -CD, we ruled out the possibility of two molecules of **2** inside the CD cavity. As can be seen in Fig. 7(c), the best fit of the model to the experimental points was obtained when unproductive complexes of both 1 : 1 and 1 : 2 stoichiometries are considered.

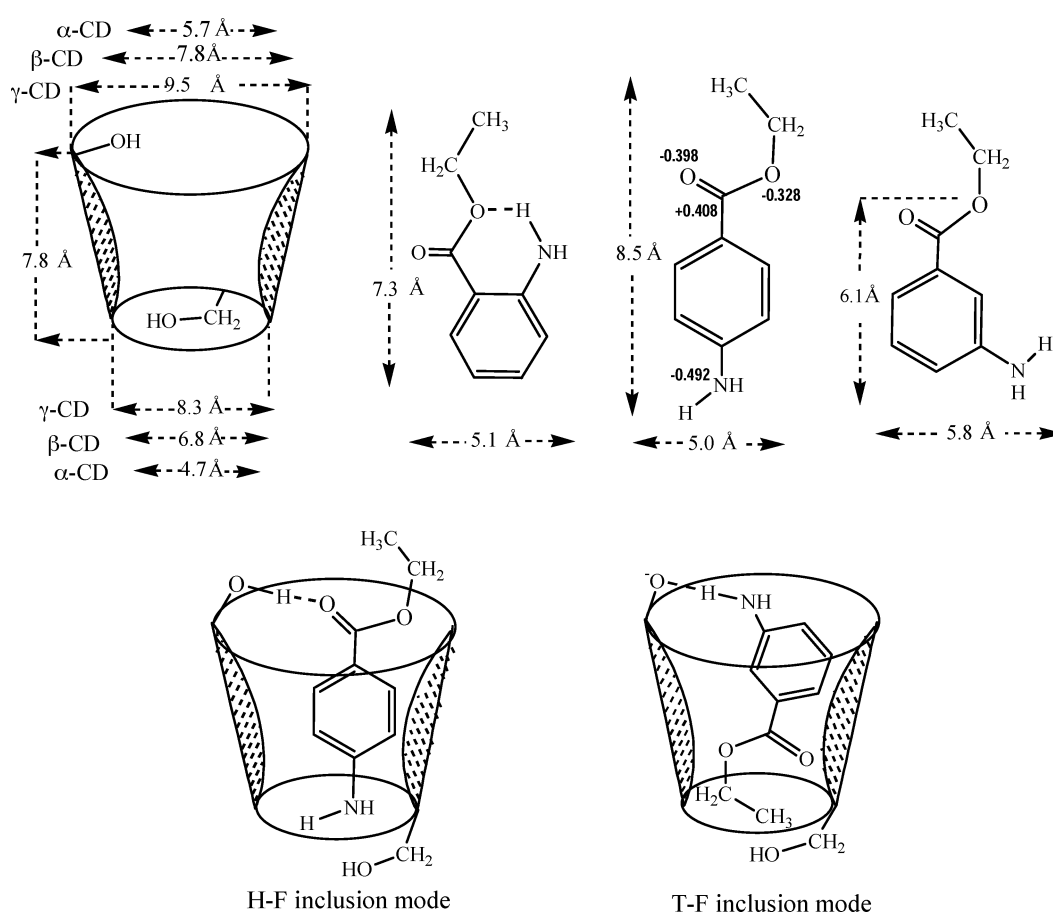
The apparently different behaviour observed with β -CD is the consequence of the smaller concentration interval used, *i.e.* the maximum $[\beta\text{-CD}]$ is nearly 5-fold lower than that used with α - or γ -CD, due to the lower solubility of β -CD. On the contrary, good agreement between the measured k_o at each $[\text{CD}]$ and the calculated values from eqn (6) is obtained in the case of the hydrolysis of **3** and **4** if one considers the formation of only 1 : 1 inclusion complexes, that is, K_{12} is negligible. The complexes formed between **4** and γ -CD showed to undergo hydrolysis at approximately half-the rate measured in water.

In alkaline conditions, the CDs have the secondary $-\text{OH}$ group ionized, *i.e.*, they are anionic hosts. Then, the hydration of the wider rim is more important in alkaline medium than in neutral or acid medium (neutral host); this fact difficult the inclusion of hydrophobic guests. In spite of that, the complex stability constants reported in Table 6 reach values close to that measured in neutral (Table 4) or acid medium (Table 5). These results can be understood if the local anesthetic inclusion mode is oriented tail-first (T-F) in alkaline medium, but head-first (H-F) in neutral or acid media, Scheme 4. The T-F inclusion mode, stabilized by strong H-bonding between the $-\text{NH}_2$ group of LA and the alkoxide group, $-\text{O}^-$, of CD, leaves the ester function inside the CD cavity, completely protected from the nucleophilic attack of HO^- . In addition, if this conformation is assumed for the binding mode of compound **2**, the hydrophobic ethyl group would remain exposed to water; therefore, a second CD molecule protecting this moiety would explain the formation of complex of 1 : 2 stoichiometry, which would be specially stable in the case of α -CD, whose narrow cavity difficult the guest protection. On the other hand, the H-F inclusion mode, stabilized by H-bonding between the ester-group of the LA and the $-\text{OH}$ group of CD, leaves the amine group protected from the nitrosating agent, XNO. The molecular geometry of benzocaine gives 'loose fit' inclusion complexes with different degree of encapsulation, mainly in the case of γ -CD host, which can be exposed to the reagents in the bulk

Table 6 Experimental conditions and results obtained in the alkaline hydrolysis of **2**, **3**, and **4** in the presence of cyclodextrins; k_w and k_c are the pseudo-first order rate constants for the hydrolysis of the free and complexed LA, respectively, and K'_{11} and K_{12} represent the stability constants on inclusion complexes of 1 : 1 and 1 : 2 (LA : CD) stoichiometry, see eqn (6)

LA (c/M)	Cyclodextrin ^a	$[OH^-]/M$	$k_w/10^{-4} s^{-1}$	$k_c/10^{-4} s^{-1}$	K'_{11}/M^{-1}	K_{12}/M^{-1}
2 (5.3×10^{-4})	α -CD (0–40) mM	0.075	3.43	—	49 ± 2	78 ± 3
	β -CD (0–9) mM	0.075	3.50	—	114 ± 2	—
	γ -CD (0–40) mM	0.095	4.16	—	34 ± 2	13 ± 3
3 (5.6×10^{-4})	α -CD (0–40) mM	0.040	12.8	—	34.0 ± 0.8	—
	β -CD (0–9) mM	0.045	14.1	—	123 ± 2	—
	γ -CD (0–40) mM	0.040	12.7	—	41.8 ± 0.8	—
4 (9×10^{-5})	α -CD (0–40) mM	0.075	2.23	—	86 ± 3	—
	β -CD (0–9) mM	0.075	2.23	—	420 ± 8	—
	γ -CD (0–15) mM	0.075	2.23	0.94 ± 0.05	140 ± 10	—

^a Cyclodextrin type and concentration interval used.



Scheme 4 Dimensions and sizes of the optimized structures of host and guest and the proposed geometries of inclusion complexes: head-first in neutral medium and tail-first in alkaline medium.

aqueous phase. The HyperChem software package was used for the geometrical optimization of the molecular structures of local anesthetics that are displayed in Scheme 4 and compared to that of cyclodextrins.

Conclusions

The results presented here indicate that ethyl 2-aminobenzoate, ethyl 3-aminobenzoate, and ethyl 4-aminobenzoate bind to

micelles – formed by either cationic or anionic surfactants – and to α -, β -, and γ -cyclodextrin showing different location sites or geometries of the inclusion complexes.

The hydrophobic local anesthetic molecules, such as ethyl 2-aminobenzoate, together with the absence of specific interactions with interfaces (*e.g.* electrostatic or hydrogen bonding), allow local anesthetics to penetrate more efficiently across hydrophobic interfaces and, by extension, across biological membranes, which redound in high anesthetic effect.

The dominant interactions – van der Waals interactions and the hydrophobic effect – observed in the complexation of local anesthetics bearing a tertiary amine moiety, such as novocaine or tetracaine, are drastically changed when specific interactions with CD are allowed. The strong hydrogen bonding between the H₂N group of LA and the alkoxide –O⁻ group of CD not only give high stable inclusion complexes, but also a change in the binding mode of the LA and even in the stoichiometry of the complex. Therefore, the complexation with cyclodextrins enhances the stability of LA, which are protected from reagents in the bulk water phase.

Acknowledgements

We are indebted to Dr Mercedes Novo of the Facultad de Ciencias, Campus de Lugo, University of Santiago de Compostela, for the time-resolved fluorescence measurements. Financial support from the Dirección General de Investigación (Ministerio de Educación y Ciencia) of Spain and FEDER (Project CTQ2005-07428/BQU) and from Dirección General de Programas y Transferencia de Conocimiento (Ministerio de Ciencia e Innovación) of Spain (Project CTQ2008-04429/BQU) is gratefully acknowledged.

References

- H. Matsuki, H. Satake, S. Kaneshina, P. R. Krishna and I. Ueda, Surface and colloid properties of local anesthetic solutions, *Curr. Topics Coll. Interface Sci.*, 1997, **2**, 69.
- P. T. Frangopol and D. Mihailescu, Interactions of some local anesthetics and alcohols with membranes, *Colloids Surf., B*, 2001, **22**, 3.
- W. C. Bowman and M. J. Rand, *Textbook of Pharmacology*, Blackwell Sci. Publs., University Press, Cambridge, 1990.
- Local Anesthetics*, Handbook of Experimental Pharmacology, ed. J. M. Ritchie and G. R. Strichartz, Springer-Verlag, Berlin, 1987, vol. 81, chap. 2.
- J. Szejtli, Cyclodextrin complexed generic drugs are generally not-bio-equivalent with the reference products: therefore the increase in number of marketed drug/cyclodextrin formulations is so slow, *J. Inclusion Phenom. Macrocyclic Chem.*, 2005, **52**, 1.
- G. Savelli, R. Germani and L. Brinchi, in *Reaction and Synthesis in Surfactant Systems*, T. Texter, ed., Marcel Dekker, Inc.: New York, 2001, vol. 100, chap. 8.
- C. A. Bunton, F. Nome, F. H. Quina and L. S. Romsted, Ion binding and reactivity at charged aqueous interfaces, *Acc. Chem. Res.*, 1991, **24**, 357.
- P. Speicer, Biological and technological relevance of amphiphilic structures in apolar medium, in *Reverse Micelles*, P. L. Luise and B. E. Straub, ed., Plenum Press: New York, 1984, pp. 339–346.
- K. A. Connors, *Measurement of cyclodextrin complex stability constants*, in *Comprehensive Supramolecular Chemistry*, J. Szejtli, T. Osa, ed. Pergamon, 1996, vol. 3, pp. 205–241.
- J. Szejtli, Cyclodextrin inclusion complexes, *Cyclodextrin Technology*, Kluwer Acad. Publishers, Netherlands, 1988, chap. 2.
- O. S. Tee, The stabilization of transition states by cyclodextrins and other catalysts., *Adv. Phys. Org. Chem.*, 1994, **29**, 1, and references therein.
- W. Saenger, Cyclodextrin inclusion compounds in research and industry, *Angew. Chem., Int. Ed. Engl.*, 1980, **19**, 344.
- N. Takisawa, K. Shirahama and I. Tanaka, Interactions of amphiphilic drugs with α -, β -, and γ -cyclodextrins, *Colloid Polym. Sci.*, 1993, **271**, 499.
- E. Iglesias, Inclusion complexation of novocaine by β -cyclodextrin in aqueous solutions, *J. Org. Chem.*, 2006, **71**, 4383.
- E. Iglesias, Investigation of physico-chemical behaviour of local anesthetics in aqueous SDS solutions, *New J. Chem.*, 2008, **32**, 517.
- I. Iglesias-García, I. Brandariz and E. Iglesias, Fluorescence study of tetracaine-cyclodextrin inclusion complexes, *Supramol. Chem.*, 2010, **22**, 228.
- B. Reija, W. Al-Soufi, M. Novo and J. Vázquez-Tato, Specific Interaction in the inclusion complexes of pyronines Y and B with β -cyclodextrin, *J. Phys. Chem. B*, 2005, **109**, 1364.
- R. Stewart, *The Proton Applications to Organic Chemistry*, Academic Press, Inc., 1985, chap. 3.
- G. S. Cox and N. J. Turro, Methyl salicylate fluorescence as a probe of the geometry of complexation to cyclodextrins, *Photochem. Photobiol.*, 1984, **40**, 185.
- A. Domínguez, A. Fernández, N. González, E. Iglesias and L. Montenegro, Determination of critical micelle concentration of some surfactants by three techniques., *J. Chem. Educ.*, 1997, **74**, 1227.
- M. V. Rekharsky and Y. Inoue, Complexation thermodynamics of cyclodextrins, *Chem. Rev.*, 1998, **98**, 1875.
- A. Ueno and T. Osa, Host-guest photochemistry in solution, in *Photochemistry in Organized and Constrained Media*, V. Ramamurthy, ed., VCH Publishers, Inc., New York, 1991, chap. 16.
- G. Krishnamoorthy and S. K. Dogra, TICT of 2-(4'-N,N-dimethylamino phenyl)pyrido[3,4-d]imidazole in cyclodextrins: Effect of pH, *J. Phys. Chem. A*, 2000, **104**, 2542.
- (a) S. Monti, L. Flamigni, A. Martelli and P. Bortolus, Photochemistry of benzophenone-CD inclusion complexes., *J. Phys. Chem.*, 1988, **92**, 4447; (b) S. Monti, G. Köhler and G. Grabner, Photophysics and photochemistry of methylated phenols in β -cyclodextrin inclusion complexes, *J. Phys. Chem.*, 1993, **97**, 13011; (c) S. Monti, G. Marconi, F. Manoli, P. Bortolus, B. Mayer, G. Grabner, G. Köhler, W. Boszczyk and K. Rotkiewicz, Spectroscopic and structural characterization of the inclusion complexes of p-dimethylaminobenzonitrile with cyclodextrins., *Phys. Chem. Chem. Phys.*, 2003, **5**, 1019; (d) S. Monti, P. Bartolus, F. Manoli, G. Marconi, G. Grabner, G. Köhler, B. Mayer, W. Boszczyk and K. Rotkiewicz, Microenvironmental effects in the excited state properties of p-dimethylaminobenzonitrile complexed to α - and β -cyclodextrin, *Photochem. Photobiol. Sci.*, 2003, **2**, 203.
- K. Takahashi, Organic reactions mediated by cyclodextrins, *Chem. Rev.*, 1998, **98**, 2013.
- E. Iglesias, Cyclodextrins as enzyme models in nitrosation and in acid-base hydrolysis reactions of alkyl nitrites., *J. Am. Chem. Soc.*, 1998, **120**, 13057.
- K. A. Connors, *Binding Constants. The Measurements of Molecular Complex Stability*, Wiley, New York, 1987, chap. 8.
- L. M. A. Pinto, L. F. Fraceto, M. H. A. Santana, T. A. Pertinhez, S. Jr. Oyama and E. Paula, Physicochemical characterization of benzocaine- β -cyclodextrin inclusion complexes, *J. Pharm. Biomed. Anal.*, 2005, **39**, 956.
- D. L. H. Williams, *Nitrosation Reactions and the Chemistry of Nitric Oxide*, Elsevier, 2004, chap. 1.
- (a) D. M. Davies and M. E. Deary, Stability of 1:1 and 2:1 α -CD-p-nitrophenyl acetate complexes and the effect of α -CD on acyl transfer to peroxide anion nucleophiles, *J. Chem. Soc., Perkin Trans. 2*, 1999, 1027; (b) E. Iglesias, Ester hydrolysis and enol nitrosation reactions of ethyl cyclohexanone-2-carboxylate inhibited by β -cyclodextrin., *J. Org. Chem.*, 2000, **65**, 6583.
- J. Szejtli, Introduction and general overview of cyclodextrin chemistry, *Chem. Rev.*, 1998, **98**, 1743.